



## OPEN

Divergent Label-free Cell Phenotypic Pharmacology of Ligands at the Overexpressed  $\beta_2$ -Adrenergic Receptors

SUBJECT AREAS:

RECEPTOR  
PHARMACOLOGY

SENSORS AND PROBES

Ann M. Ferrie\*, Haiyan Sun\*†, Natalya Zaytseva &amp; Ye Fang

Received  
12 September 2013Accepted  
6 January 2014Published  
23 January 2014Correspondence and  
requests for materials  
should be addressed to  
Y.F. (fangy2@corning.  
com)\* These authors  
contributed equally to  
this work.† Current address:  
Bioscience Institute,  
Arizona State  
University, AZ 85287,  
USA.

Biochemical Technologies, Science and Technology Division, Corning Incorporated, Corning, NY 14831, United States of America.

We present subclone sensitive cell phenotypic pharmacology of ligands at the  $\beta_2$ -adrenergic receptor ( $\beta_2$ -AR) stably expressed in HEK-293 cells. The parental cell line was transfected with green fluorescent protein (GFP)-tagged  $\beta_2$ -AR. Four stable subclones were established and used to profile a library of sixty-nine AR ligands. Dynamic mass redistribution (DMR) profiling resulted in a pharmacological activity map suggesting that HEK293 endogenously expresses functional  $G_i$ -coupled  $\alpha_2$ -AR and  $G_s$ -coupled  $\beta_2$ -AR, and the label-free cell phenotypic activity of AR ligands are subclone dependent. Pathway deconvolution revealed that the DMR of epinephrine is originated mostly from the remodeling of actin microfilaments and adhesion complexes, to less extent from the microtubule networks and receptor trafficking, and certain agonists displayed different efficacy towards the cAMP-Epac pathway. We demonstrate that receptor signaling and ligand pharmacology is sensitive to the receptor expression level, and the organization of the receptor and its signaling circuitry.

G protein-coupled receptors (GPCRs) represent the largest class of drug targets, owing to their important regulatory roles in virtually all physiological processes as well as their accessibility to therapeutic inventions<sup>1,2</sup>. GPCRs can activate several G protein isoforms, and also signal through G protein-independent pathways<sup>3,4</sup>. Many receptor ligands often have distinct efficacy profiles toward different signaling pathways downstream the receptor<sup>5-7</sup>. This is exemplified by ligands acting at the  $\beta_2$ -adrenergic receptor ( $\beta_2$ -AR), a prototypic  $G_s$ -coupled receptor<sup>8-23</sup>. Pharmacological assays based on the measurement of individual molecules in the  $\beta_2$ -AR signaling pathways have revealed that some ligands such as carvedilol and propranolol preferentially activate  $\beta$ -arrestin pathway over cyclic AMP (cAMP) pathway<sup>9,12-13</sup>; consequently, many receptor ligands often have pluridimensional efficacy<sup>11</sup>. This “biased agonism” is believed to be originated from the intrinsic conformational plasticity of a receptor protein, in that the receptor exist as collections (termed “ensembles”) of tertiary conformations and constantly samples these conformations according to changes in the thermal energy in the system<sup>4</sup>. Increasing evidence suggests that the  $\beta_2$ -AR exists multiple ligand-specific and functional conformations<sup>24-32</sup>. Ligands can stabilize specific conformations of the receptor mostly likely through conformational selection, in which an agonist would bind reversibly to diverse conformations in the receptor ensemble to a similar extent, and the receptor-agonist complex is stabilized only when the ligand binding to certain conformational intermediates is more favorable over others<sup>33</sup>. The product of this thermodynamic process is the operational bias of functionally distinct ligands to allosterically turn on certain signaling proteins, and thus activate different cell signaling processes.

However, quantifying biased agonism is challenging. The ligand bias that is thought to be therapeutically important is often complicated by system and observational bias<sup>34,35</sup>. The system bias is due to the relative efficiency with which different pathways may be coupled to signaling proteins in the cell, while the observational bias is originated from the sensitivity of different assays to measure the response of the cells to agonist stimulation<sup>35</sup>. Since all agonists are subject to the same signaling circuitry presented by the cell system, as well as to the same experimental conditions used in the assays, both system and observational bias are considered to be useless for gaining therapeutic advantage<sup>35</sup>. However, given that the receptor conformations can be regulated allosterically by cell membrane constituents and intracellular signaling proteins<sup>4</sup>, the system bias can be leveraged to manifest the biased agonism in the context of self-referenced pharmacological activity map.

In the recent years, label-free resonant waveguide grating (RWG) biosensor has become increasingly popular for profiling ligand-receptor interactions in both native and recombinant cells. These biosensors can translate the functional consequences of a ligand-receptor interaction in living cells into a real-time and integrated cell



phenotypic response, termed dynamic mass redistribution (DMR)<sup>36–38</sup>. The DMR signal arising from a ligand-receptor interaction enables analysis of the systems cell biology of the receptor using chemical biology tools<sup>38–40</sup>, and allows for pharmacological classification of ligands with high-resolution<sup>41–44</sup>. Herein, we compare the label-free cell phenotypic activities of a library of sixty-nine AR ligands in the parental human embryonic kidney (HEK293) cell line with those in the four subclones of its engineered cells, all of which stably express green fluorescent protein (GFP) tagged  $\beta_2$ -ARs (HEK- $\beta_2$ AR-GFP). Combining with pathway deconvolution using probe molecules and RNA interference (RNAi) against key signaling proteins, we have found that the AR ligands tested display divergent cell phenotypic pharmacology.

## Results

**Generation of HEK- $\beta_2$ AR-GFP subclones.** HEK293, widely used for studying the signaling bias of ligands acting at both endogenous and recombinant  $\beta_2$ -ARs, was selected to generate stable clones bearing the  $\beta_2$ AR-GFP. HEK293 is known to endogenously express the  $\beta_2$ -AR with a level of 30 to 40 fmol/mg membrane protein<sup>45</sup>. Four stable subclones A to D of HEK- $\beta_2$ AR-GFP cells were established through single cell cloning through transfecting the parental cells with human pCMV- $\beta_2$ AR-GFP plasmid and subsequent selection with the aminoglycoside G418. These subclones were selected based on the GFP expression level (Fig. 1). The epi-fluorescence image showed that the  $\beta_2$ -AR protein in the subclone A is mostly expressed at the cell plasma membrane (Fig. 1a). The total internal reflection

microscopic imaging further showed that the  $\beta_2$ AR-GFP is mostly uniformly distributed within the basal cell membrane with higher density near the cell peripheral area (Fig. 1b). Flow cytometry analysis showed that the fluorescence intensity is in the order of subclone A > subclone C ~ subclone D > subclone B, while it is the most uniform for the subclone A (Fig. 1c–f). Given its high and uniform GFP fluorescence, we primarily compared the pharmacology and signaling of AR ligands in the subclone A with the parental HEK293.

**Label-free cell phenotypic activity map of AR ligands.** To characterize the cell phenotypic pharmacology of ligands, we first prepared a library of sixty-nine AR ligands consisting of known ligands for all nine family members of the adrenergic receptors (Supplementary Table S1). To achieve maximal signaling capacity and to be amenable for high throughput screening, we then profiled all ligands, each at 10  $\mu$ M with four replicates across the five cell lines. For effective similarity analysis<sup>42–44</sup>, the averaged DMR signal of each ligand in an assay was then translated to a six-dimensional coordinate; that is, the real DMR responses at six distinct time points including 3, 5, 9, 15, 30 and 45 min post stimulation. Therefore, the five DMR signals of each ligand in the five cell lines were rewritten into a thirty dimensional coordinate. For each cell line we included both positive (that is, epinephrine) and negative (that is, the assay buffer containing equal amount of DMSO) controls to define the range of responses for classification of ligand agonism. Ligands whose DMR were smaller than 30 pm (picometer shift in the resonant wavelength of the biosensor) and similar to the negative

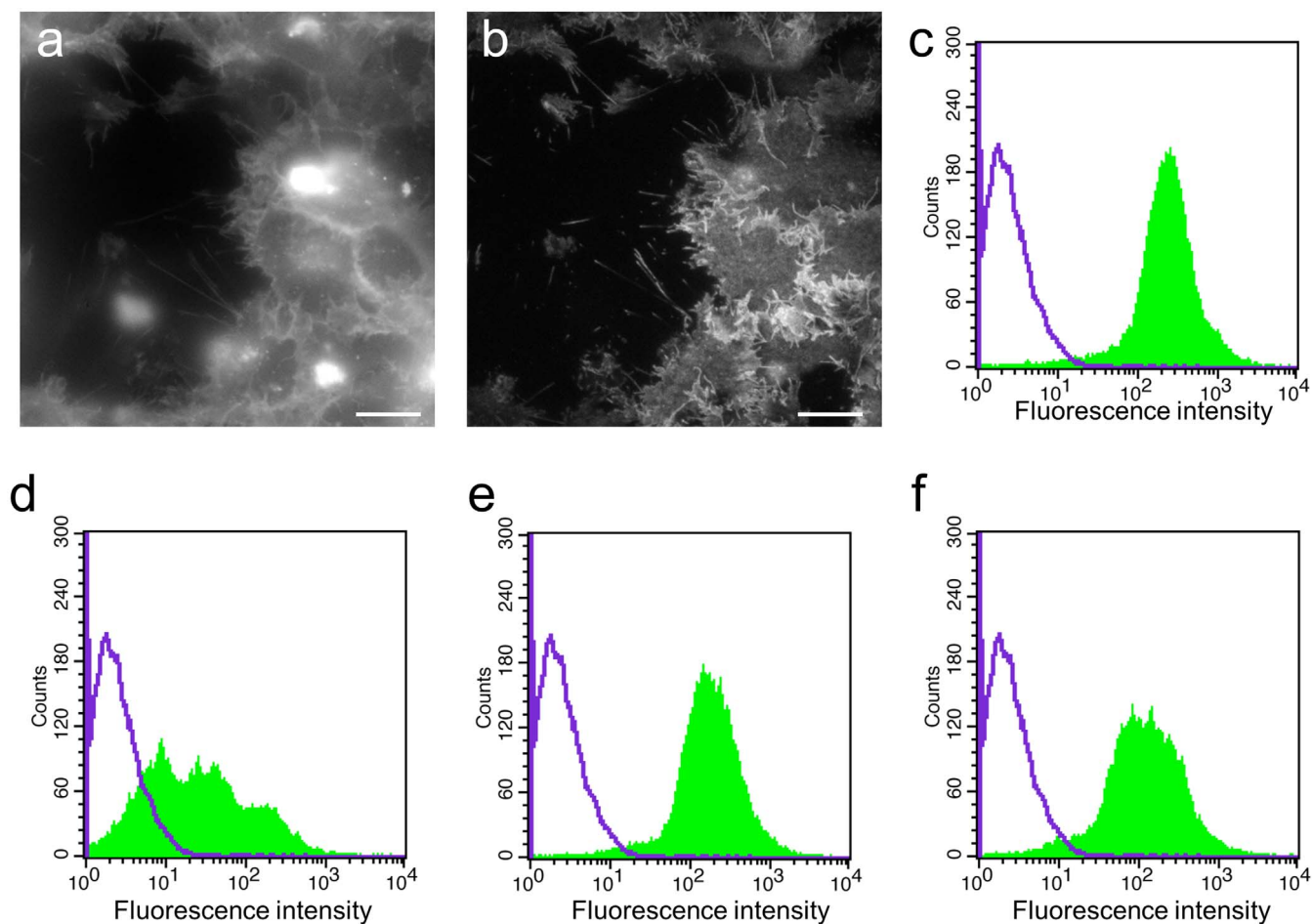


**Figure 1 | Fluorescence analysis of the HEK- $\beta_2$ AR-GFP cells.** (a) Epi-fluorescence of the subclone A; (b) TIRF image of the subclone A; (c–f) Flow cytometry histogram of subclone A (c), B (d), C (e), and D (f), in comparison with the parental cell line (purple line). For (a,b) the cells were cultured on glass substrate and directly imaged without fixation. Scale bar in a, b is 10  $\mu$ m. For (c–f) total 30,000 events were counted for each cell line.

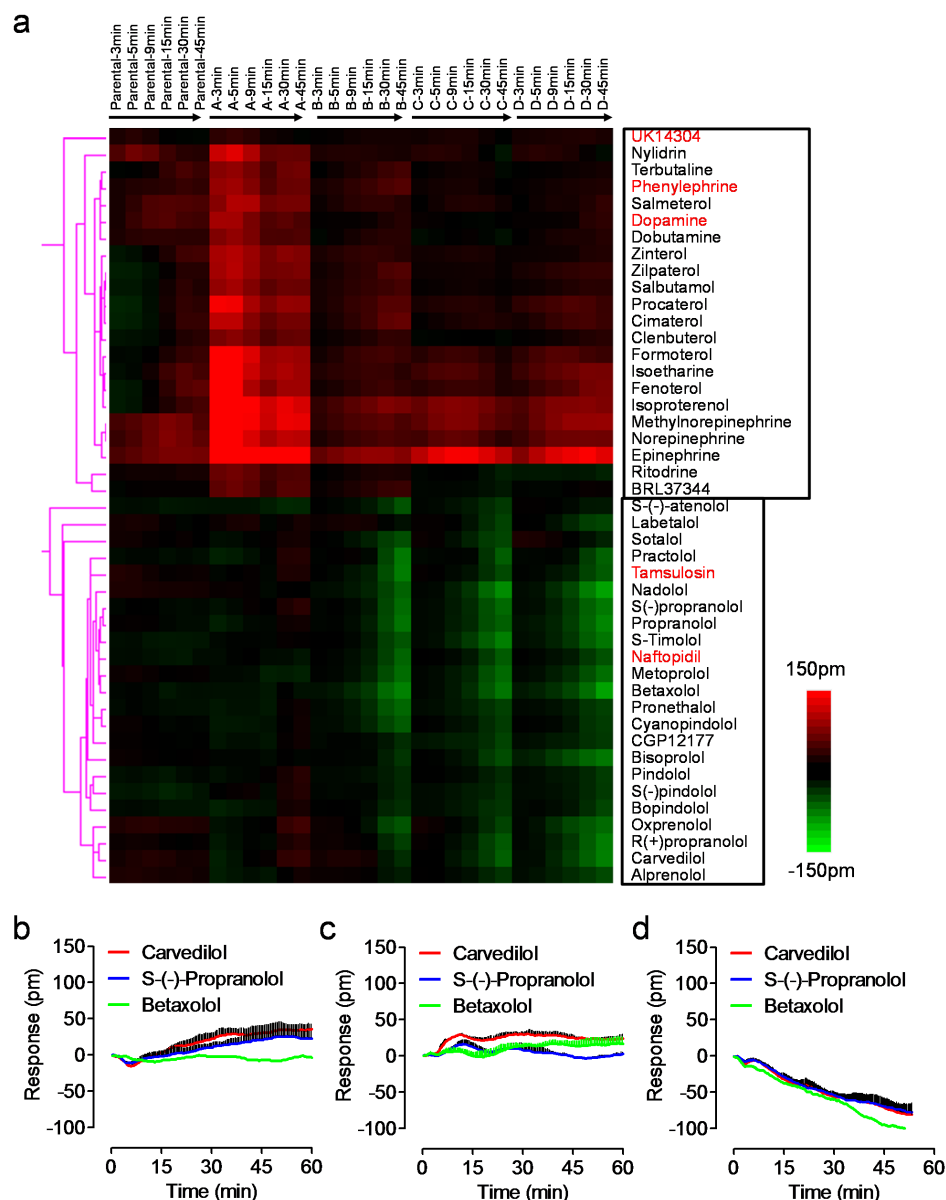


**Figure 2** | DMR agonist heatmap of AR ligands in the five cell lines. (a) The heat map obtained using DMR agonist profiling of the ligands in the five cell lines, followed by similarity analysis using the Ward hierarchical clustering algorithm and Euclidean distance metrics. The cell lines from left to right were the parental HEK293 (Parental), and the four stable subclones (A, B, C, D). For each ligand in a cell line, its real DMR responses at six time points (3, 5, 9, 15, 30, and 45 min post stimulation) were grouped together in a time series from left to right, so its kinetic signature can be directly visualized. False colored scale bar is included to assist the data visualization. Only forty-five active ligands were included in this analysis, given that the remaining twenty-four ligands did not trigger any detectable DMR in any of the five cell lines. (b–d) The DMR of three antagonists, betaxolol, carvedilol, and S(-)-propranolol, each at 10  $\mu$ M, in untreated subclone A (b), Epac1 RNAi-treated subclone A (c), or untreated subclone D (d).

controls across all cell lines were considered to have no agonist activity and excluded from similarity analysis. Results showed that forty-five out of the sixty-nine ligands were found to trigger detectable DMR in at least one of the five cell lines (Fig. 2).

Similarity analysis using unsupervised Ward hierarchical clustering algorithm and Euclidean distance metrics<sup>46</sup> categorized ligands into distinct clusters (Fig. 2). Several interesting features emerged. First, the active ligands were classified into two large clusters. The first one constitutes of known agonists including epinephrine and generally led to a positive DMR signal when being active in a cell line. The second cluster comprises of antagonists including propranolol and generally resulted in a negative DMR signal in the recombinant subclones B to D. Second, the active ligands are mostly  $\beta$ -AR-selective. Out of the forty-five active ligands, only the  $\alpha_2$ -AR-selective full

agonist UK14,304 and the  $\alpha_1$ -AR-selective antagonist tamsulosin were unknown for their activity acting at the  $\beta_2$ -AR. Both phenylephrine and dopamine are known to have agonist activity at the  $\beta_2$ -AR with relatively low potency<sup>47</sup>, while another  $\alpha_1$ -AR-selective antagonist naftopidil was reported to bind to the  $\beta_2$ -AR with a  $K_i$  of 1  $\mu$ M<sup>48</sup>. Third, among all beta-blockers examined, only acebutolol was inactive in all cell lines. Interestingly, compared to betaxolol that was inactive, carvedilol and propranolol both triggered a small and slowly increased DMR in the subclone A (Fig. 2b), which were sensitive to exchange proteins activated by cAMP (EPAC) RNAi knockdown (Fig. 2c). In contrast, all three antagonists triggered similar negative DMR in the subclone D (Fig. 2d). Nonetheless, the activity map obtained suggests that the cell phenotypic pharmacology of AR ligands is dependent on the subclones generated from a single transfection batch.

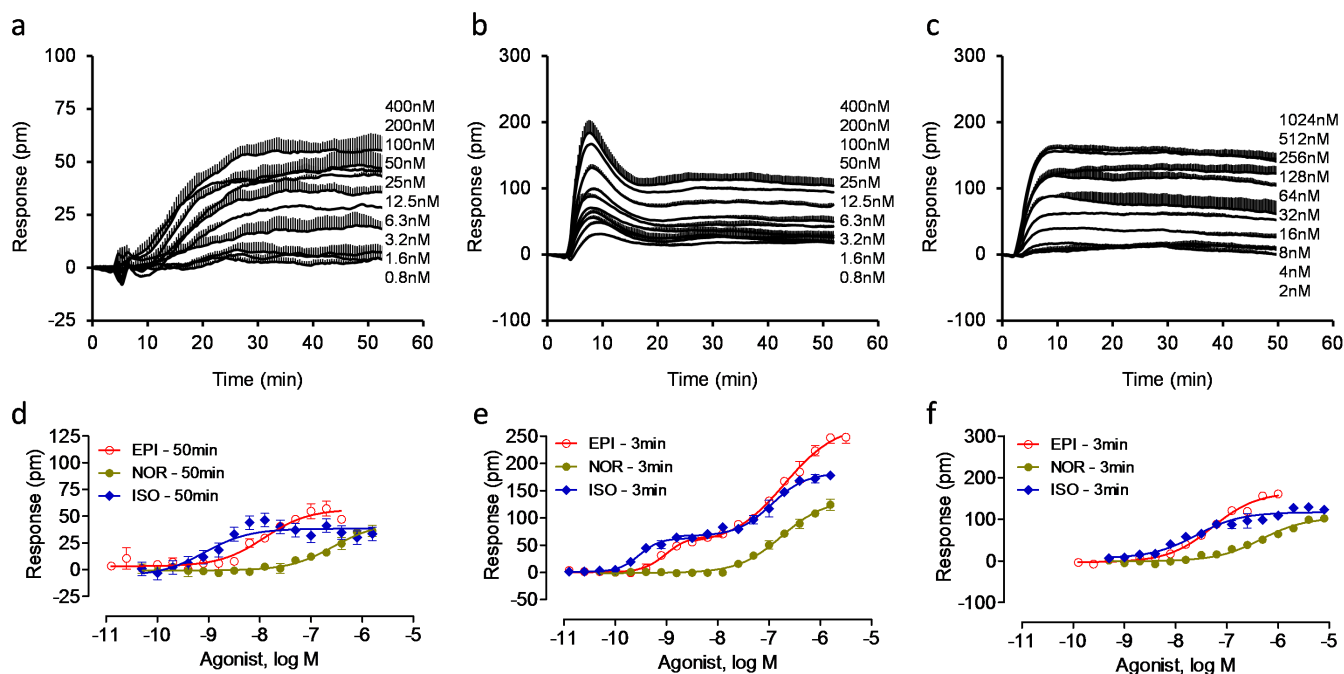


**Figure 3** | The DMR dose responses of epinephrine in three different cell lines. (a–c) Real time DMR dose responses of epinephrine in the parental HEK293 (a), subclone A (b), and subclone D (c). (d–f) The DMR amplitudes at 50 min as a function of agonist doses in the parental HEK293 (d), subclone A (e), and subclone D (f). EPI: epinephrine; NOR, norepinephrine; ISO, isoproterenol. Data represents mean  $\pm$  s.d. ( $n = 4$ ) for all.

**Receptor subtype specificity of epinephrine.** Next, we determined the receptor subtype specificity of the epinephrine-induced responses given that epinephrine is a non-selective endogenous agonist for all ARs. First, we examined the dose responses of three agonists, epinephrine, norepinephrine, and isoproterenol, in the parental line and two representative clones (A and D). Results showed that all dose responses were cell line dependent (Fig. 3). In general, the maximal signal was the greatest in the subclone A and the lowest in the parental line, consistent with the expression level of the receptor. All three agonists triggered a sustained positive DMR in the three cell lines; however, their early responses showed the greatest divergence in characteristics (Fig. 3a–c). The dose responses were monophasic in the parental and subclone D cells for all three agonists, but were monophasic for norepinephrine and biphasic for both epinephrine and isoproterenol in the subclone A (Fig. 3d–f). Furthermore, all three agonists also gave rise to cell line-dependent potency (Table 1). For each agonist its potency was generally in the order of subclone A > parental > subclone D. For all three agonists in the subclone A their potency was higher when the stimulation duration is longer; however, in the subclone D their potency was mostly insensitive to the stimulation duration. These results suggest that the cell phenotypic pharmacology of agonists is sensitive to the receptor expression level.

Second, we examined the ability of distinct ligands to block or desensitize the DMR of epinephrine in both the parental line and subclone A using a two-step DMR antagonist/desensitization assay,

each lasting  $\sim 1$  hr<sup>23</sup>. All ligands were assayed at a single dose (10  $\mu$ M) with four replicates, and were presented throughout the assay. The epinephrine DMR in the second step was recalculated after re-established the baseline 3 min before the epinephrine stimulation. Similarity analysis using the ligand-induced DMR and the epinephrine DMR in the presence of the ligand resulted in an interesting map shown in Supplementary Figure S1, which was far more complicated than the agonist activity map shown in Fig. 2. Almost all ligands modulated the epinephrine DMR but to different degrees –  $\beta$ -selective ligands generally led to greater suppression, while  $\alpha$ -selective ligands mostly suppressed its early response.

Detailed analysis further revealed that the parental HEK293 also has a functional  $\alpha_2$ -AR, beside the  $\beta_2$ -AR. First, the  $\alpha_1$ -agonist and  $\alpha_2$ -antagonist cirazoline<sup>49</sup> did not trigger any DMR, but selectively suppressed the early response of epinephrine; the similar was found for the  $\alpha_{1/2}$ -nonselective antagonist prazosin, suggesting that the early epinephrine response has a positive component arising from the activation of  $\alpha$ -receptor(s) (Fig. 4a). However, the potent  $\alpha_1$ -antagonist and weak  $\beta_2$ -AR binder naftopidil<sup>48</sup> was inactive in HEK293, but partially suppressed the epinephrine response; the similar was true for tamsulosin (Fig. 4b), suggesting that similar to naftopidil tamsulosin may also be a weak  $\beta_2$ -AR antagonist. Second, among all  $\alpha_2$ -selective agonists examined only UK14304 triggered a small, rapid and transiently positive DMR, but suppressed selectively the early response of epinephrine (Fig. 4c), suggesting that the early epinephrine response has a positive component arising from

**Table 1** | The subclone and stimulation time dependent potency (pEC<sub>50</sub>, mean  $\pm$  s.e.,  $n = 4$ ) of three AR agonists

	Time	Parental	Subclone A	Subclone D
Isoproterenol	3 min		$-6.96 \pm 0.06, -9.53 \pm 0.04$	$-7.60 \pm 0.12$
	50 min	$-9.07 \pm 0.20$	$-7.76 \pm 0.18, -10.29 \pm 0.16$	$-7.68 \pm 0.10$
Epinephrine	3 min		$-6.75 \pm 0.06, -9.01 \pm 0.05$	$-7.25 \pm 0.12$
	50 min	$-7.96 \pm 0.06$	$-6.86 \pm 0.06, -9.38 \pm 0.10$	$-7.19 \pm 0.18$
Norepinephrine	3 min		$-6.75 \pm 0.06$	$-6.33 \pm 0.08$
	50 min	$-6.56 \pm 0.09$	$-7.05 \pm 0.14$	$-5.93 \pm 0.06$



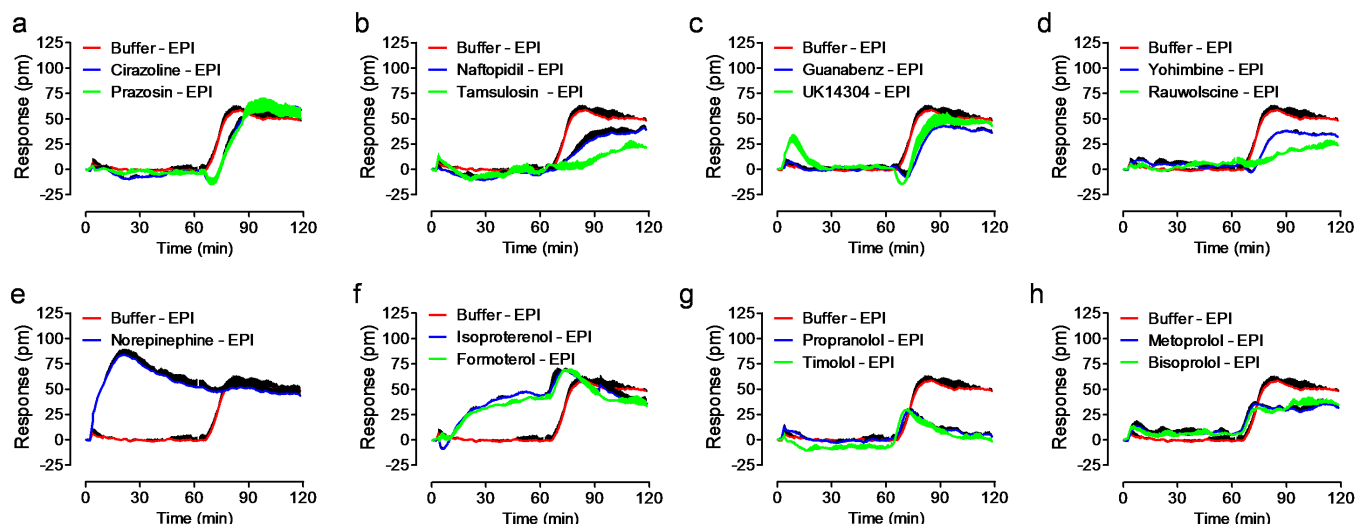


**Figure 4** | DMR characteristics of the parental HEK293 cells responding to a sequential treatment with different ligands at 10  $\mu\text{M}$  (Step 1) and 500 nM epinephrine (EPI, step 2). (a) Cirazoline and prazosin; (b) naftopidil and tamsulosin; (c) guanabenz and UK14,304; (d) yohimbine and rauwolfscine; (e) norepinephrine; (f) isoproterenol and formoterol; (g) propranolol and timolol; (h) metoprolol and bisoprolol. The DMR of cells that were first treated with the buffer vehicle followed by 500 nM EPI (Buffer – EPI) was used as the positive controls for (a–h). The EPI concentration for the second step was 500 nM ( $\sim 1 \times \text{EC}_{100}$ ). In this two-step assay, the first ligand was presented when EPI was added. Data represents mean  $\pm$  s.d. ( $n = 4$ ).

the activation of  $\alpha_2$ -receptor. This was further confirmed by  $\alpha_2$ -selective antagonist yohimbine (Fig. 4d). Notably, another  $\alpha_2$ -blocker rauwolfscine partially suppressed the entire response of epinephrine via an unknown mechanism (Fig. 4d). Third, three non-selective AR agonists including epinephrine, norepinephrine and methylnorepinephrine all triggered similar DMR, and completely desensitized the epinephrine response (Fig. 4e), suggesting that all three agonists activate both  $\alpha_2$  and  $\beta_2$ -receptors. Fourth,  $\beta$ -agonists including isoproterenol and formoterol triggered a DMR distinct from epinephrine, but only desensitized the late response of epinephrine (Fig. 4f). Furthermore, potent  $\beta_{1/2}$ -blockers including propranolol and timolol also selectively blocked the late response of epinephrine (Fig. 4g), while  $\beta$ -blockers including metoprolol and

bisoprolol that are known to be less potent at the  $\beta_2$ -AR only partially suppressed the late response of epinephrine (Fig. 4h). These results are consistent with our recent quantitative real-time PCR results showing that the parental HEK293 expresses mRNA of  $\beta_2$  (cycle threshold, 26.0)  $>$   $\alpha_{2C}$  (26.5)  $>$   $\beta_1$  (27.2)  $>$   $\alpha_{2A}$  (29.2)  $>$  other AR subtypes<sup>50</sup>.

Almost identical trend was observed in the subclone A (Fig. 5), except for that the epinephrine response is dominant by the activation of the overexpressed  $\beta_2$ -AR. The notable difference was that tamsulosin potentiated the epinephrine response via an unknown mechanism. Together, these results are the best explained by the co-expression of functional  $\alpha_{2C}$ -AR and  $\beta_2$ -AR, and the activation of the  $\alpha_{2C}$ -AR contributes selectively to the early response of epinephrine.

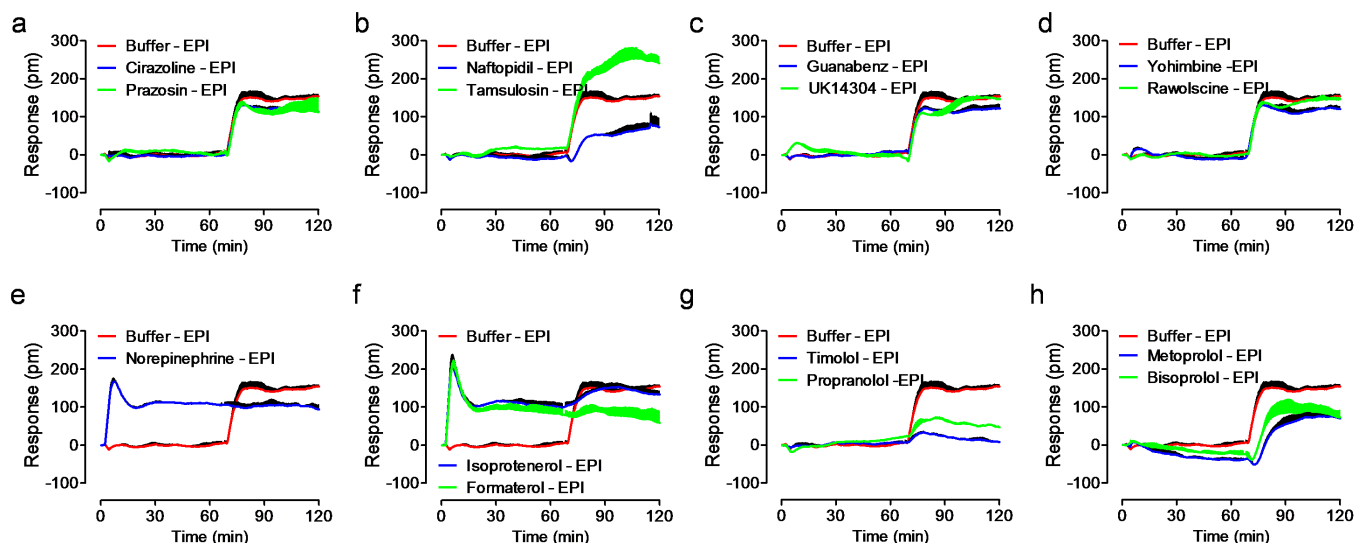


**Figure 5** | DMR characteristics of the subclone A cells responding to a sequential treatment with different ligands at 10  $\mu\text{M}$  (Step 1) and 500 nM epinephrine (EPI, step 2). (a) Cirazoline and prazosin; (b) naftopidil and tamsulosin; (c) guanabenz and UK14,304; (d) yohimbine and rauwolfscine; (e) norepinephrine; (f) isoproterenol and formoterol; (g) propranolol and timolol; (h) metoprolol and bisoprolol. The DMR of cells that were first treated with the buffer vehicle followed by 500 nM EPI (Buffer – EPI) was used as the positive controls for (a–h). All ligands were assayed at 10  $\mu\text{M}$  with four replicates. The EPI concentration for the second step was 500 nM ( $\sim 1 \times \text{EC}_{100}$ ). In this two-step assay, the first ligand was presented when EPI was added. Data represents mean  $\pm$  s.d. ( $n = 4$ ).

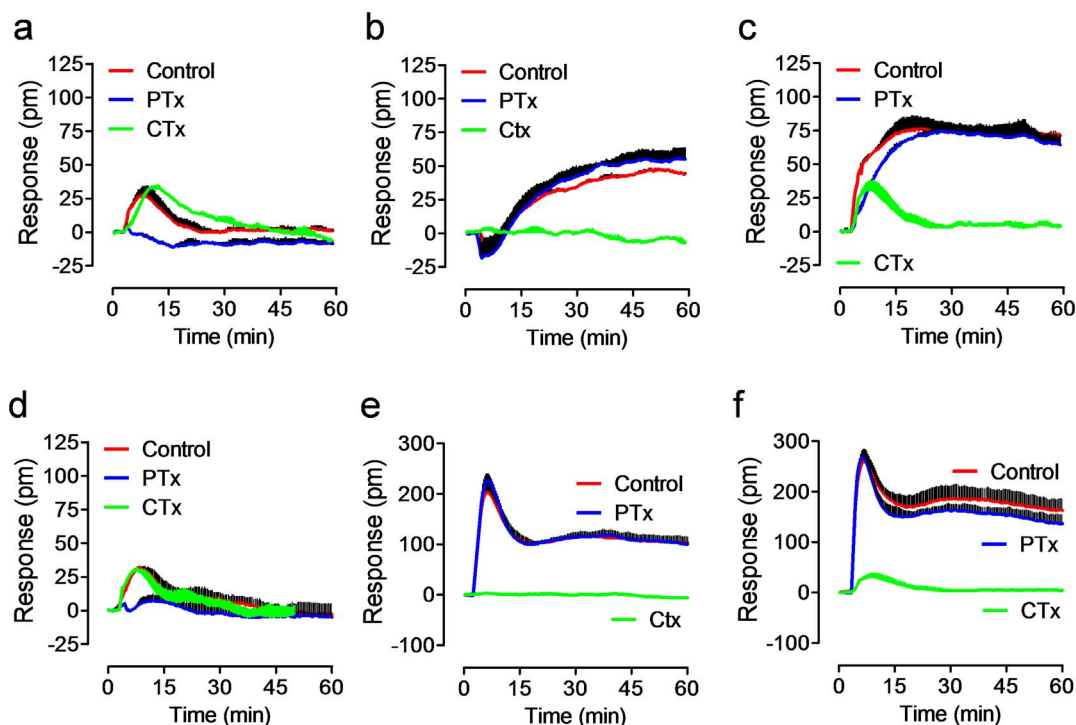


**Figure 6** | Real-time DMR of AR agonists in different cell lines without (control) or with CTx or PTx pretreatment. (a–c) The parental HEK293 cells; (d–f) the subclone A cells. (a,d) 10  $\mu$ M UK14304; (b,e) 10  $\mu$ M isoproterenol; (c,f) 10  $\mu$ M epinephrine. Data represents mean  $\pm$  s.d. (n = 4).

**G protein pathway analysis.** Given that  $\alpha_{2c}$ -AR is a  $G_{\alpha i}$ -coupled receptor and  $\beta_2$ -AR is a prototypic  $G_{\alpha s}$ -coupled receptor, we next examined the G protein pathways. For the parental cell line, the permanent inhibition of  $G_{\alpha i}$  by ADP ribosylation of a cysteine of the protein with pertussis toxin (PTx) completely blocked the DMR of UK14304 (Fig. 6a), but had little impact on the isoproterenol DMR (Fig. 6b), and selectively suppressed the early DMR of epinephrine (Fig. 6c). In contrast, the permanent activation of  $G_{\alpha s}$  by ADP ribosylation of an arginine residue of the protein by chorea toxin (CTx) had little impact on the UK14304 DMR (Fig. 6a), but completely blocked the isoproterenol DMR (Fig. 6b), and selectively blocked the late response of epinephrine (Fig. 6c). Almost identical trend was observed in the subclone A (Fig. 6d–f). These results suggest that the activation of the  $\alpha_{2c}$ -AR triggers  $G_{\alpha i}$  signaling, while the activation of the  $\beta_2$ -AR leads to  $G_{\alpha s}$  signaling. These results also suggest that epinephrine activates both receptors, and the  $G_{\alpha i}$  signaling via the  $\alpha_{2c}$ -AR contributes to its early DMR, but the  $G_{\alpha s}$  signaling via the  $\beta_2$ -AR contributes to its late response.

**The origin of the epinephrine response.** To characterize the origin of cellular events underlined the epinephrine DMR we examined its sensitivity to probe molecules targeting several cellular proteins in three cell lines including the parental line, and subclones A and D. First, the actin disruptor latrunculin A completely blocked the epinephrine responses in all three cell lines (Fig. 7a–c), suggesting that actin remodeling is the primary event contributing to the epinephrine DMR. Second, nocodazole and vinblastine, the two microtubule disrupting agents, had little effect on the epinephrine DMR in the parental line (Fig. 7d), but markedly increased it in the subclone D (Fig. 7e), and suppressed it in the subclone A (Fig. 7f). These results suggest that microtubule remodeling was not part of the epinephrine response detected in the parental cells, but played differential roles in the two subclones. Third, the Rho kinase inhibitor Y27632 partially suppressed the epinephrine responses in all three cell lines (Fig. 7g–i), suggesting that Rho kinase activity is important to the epinephrine responses. Fourth, the focal adhesion

kinase inhibitor PF573228 suppressed the epinephrine responses to different degree in the three cell lines (Fig. 7j–l), suggesting that the remodeling of cell adhesion complexes also contributes to the epinephrine responses. Together, these results suggest that the epinephrine responses in different cell lines are mostly due to the remodeling of actin filaments and cell adhesion complexes, and to less extent the microtubule remodeling. These results further suggest that the exact cellular mechanisms underlined the epinephrine responses in different clones are sensitive to the receptor expression level, which may in turn result in different organization and compartmentalization of signaling proteins and/or complexes.

**The effect of receptor trafficking.** DMR is an integrated cellular response upon the activation of a receptor, and is mostly due to remodeling of microfilaments, cell adhesion and morphology, as well as protein trafficking, all of which are believed to cause significant mass redistribution<sup>36–38,50–52</sup>. Given that GPCR kinases (GRKs) and  $\beta$ -arrestins are known to play important roles in receptor trafficking, we next examined the sensitivity of the epinephrine DMR to the RNAi knockdown of GRKs and  $\beta$ -arrestins in the subclone A. Western blotting showed that this cell line expresses GRK2, GRK3, and GRK6, to less extent GRK5, as well as  $\beta$ -arrestin 1/2 (Fig. 8a). RNAi knockdown experiments showed that RNAi against GRK2 markedly reduced the protein level of GRK2 and GRK6, to less extent GRK3, while RNAi against GRK3 markedly reduced the GRK3/5 protein and to less extent the GRK2/6 proteins, RNAi against GRK5 markedly reduced the GRK5/6 protein and to less extent the GRK3 protein, RNAi against GRK6 markedly suppressed GRK6 and GRK2/5. Furthermore, the two RNAi for  $\beta$ -arrestin-1 and 2 also markedly knocked down the protein levels of  $\beta$ -arrestins (Fig. 8a), although the selectivity of both RNAi is unknown due to the poor resolution of western blot and the use of non-selective anti-arrestin antibody. Nonetheless, the efficiency of RNAi knockdown was found to be about 60–75% for their intended targets.

DMR profiling results showed that as the control the mock transfection had little effect on the epinephrine response (Fig. 8b). Two

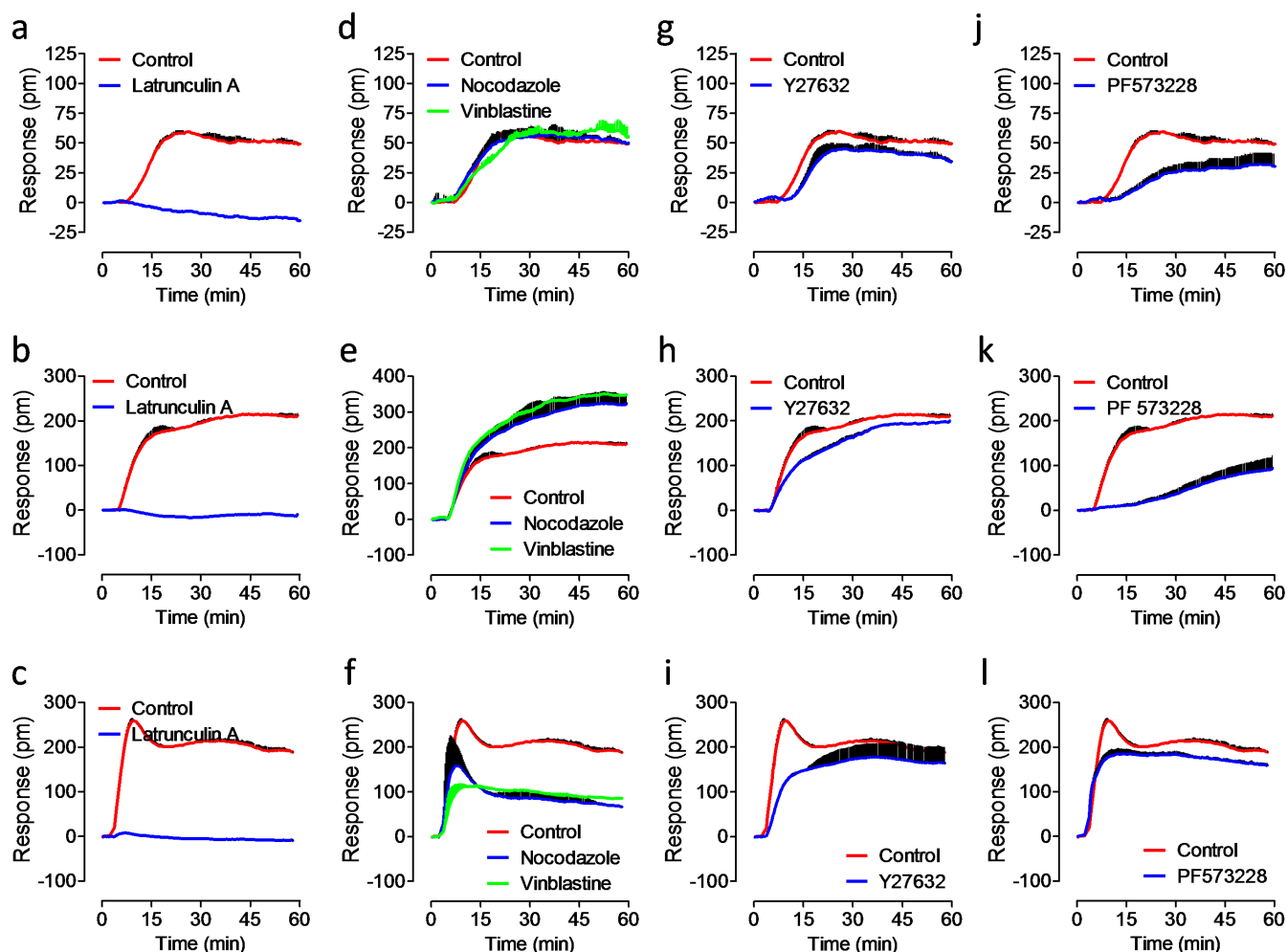


**Figure 7** | Real-time DMR of 500 nM epinephrine in different cell lines without (control) or with small probe molecule pretreatment. (a–c) 10  $\mu$ M latrunculin A; (d–f) 10  $\mu$ M nocodazole and 10  $\mu$ M vinblastine; (g–i) 10  $\mu$ M Y27632; (j–l) 10  $\mu$ M PF573228. (a,d,g,i) The parental HEK293 cells; (b,e,h,k) The subclone B; (c,f,i,l) The subclone A. The epinephrine concentration was 500 nM for all three cell lines (all  $\sim 1 \times EC_{100}$ ). Data represents mean  $\pm$  s.d. (n = 4).

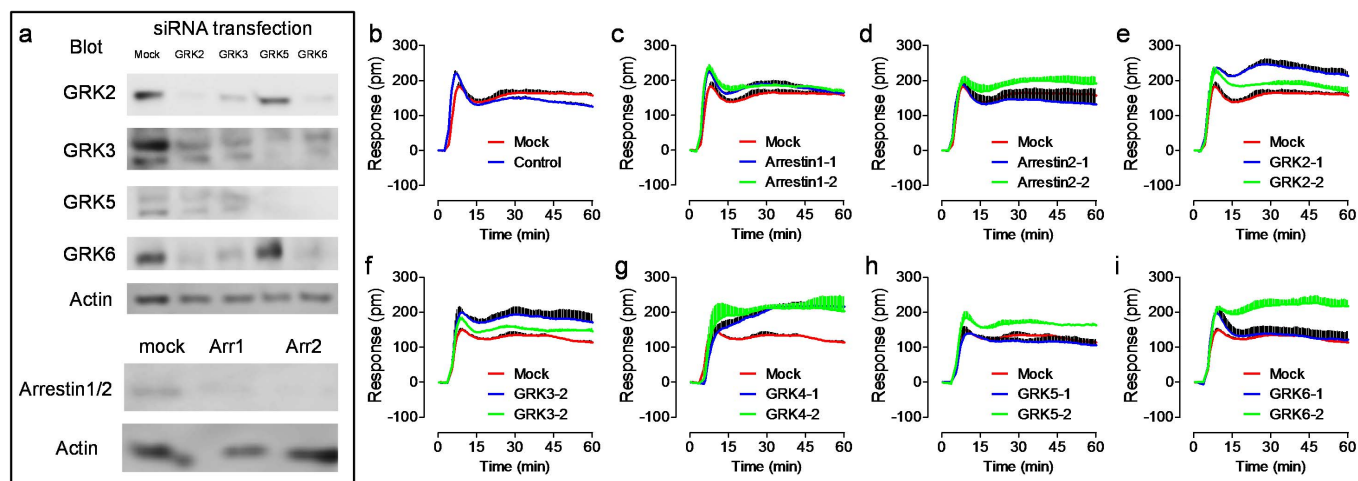


**Figure 8** | RNAi knockdown of  $\beta$ -arrestins and GRKs on the DMR of 500 nM epinephrine in the subclone A. (a) Western blots of GRKs and  $\beta$ -arrestins without (mock) or with RNAi knockdown. Actin was used as the control. (b–i) The real-time DMR of epinephrine in transfected cells: (b) mock transfection in comparison with no transfection; (c) RNAi arrestin1\_1 and arrestin1\_2; (d) RNAi arrestin2\_1 and arrestin2\_2; (e) RNAi GRK2\_1 and GRK2\_2; (f) RNAi GRK3\_1 and GRK3\_2; (g) RNAi GRK4\_1 and GRK4\_2; (h) RNAi GRK5\_1 and GRK5\_2; (i) RNAi GRK6\_1 and GRK6\_2. (b–i) Data represents mean  $\pm$  s.d. (n = 4).

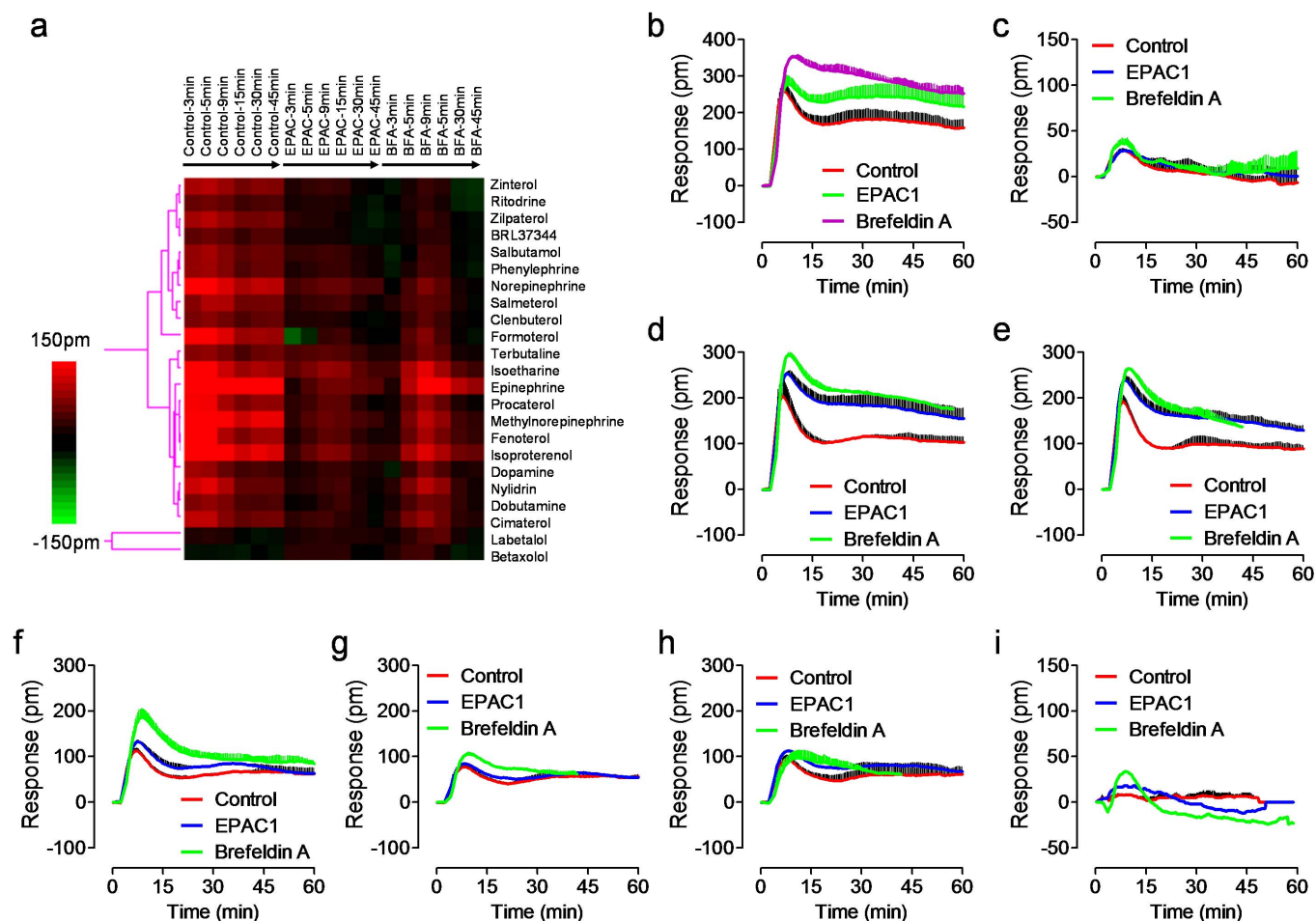


**Figure 9 | The effect of Epac inhibition on the DMR of different ligands.** (a) DMR heatmap of AR ligands in the subclone A and in the 20  $\mu$ M brefeldin A (BFA)- and RNAi Epac1-treated cells. The real responses of all ligands in the untreated cells were used for visualizing their DMR characteristics, while the treatment-induced net changes were used for better visualization of the effect of Epac inhibition. Only ligands that gave rise to a DMR of  $>40$  pm or an Epac inhibition-induced net change of  $>40$  pm were included in this analysis. (b–i) The real-time DMR of different ligands in cells without (control) or with brefeldin A- or Epac1 RNAi pretreatment: (b) epinephrine; (c) UK14,304; (d) isoproterenol; (e) Isoetharine; (f) cimaterol; (g) clenbuterol; (h) salbutamol; (i) betaxolol. All ligands were profiled at 10  $\mu$ M. Data represents mean  $\pm$  s.d. ( $n = 4$ ).

RNAi for  $\beta$ -arrestin-1 only marginally increased the epinephrine response (Fig. 8c); the similar was found for one of the two RNAi for  $\beta$ -arrestin-2 (Fig. 8d), suggesting that the  $\beta$ -arrestin-associated cellular events had small contribution to the overall response under the assay condition. In contrast, most RNAi for GRKs caused a clear increase of the epinephrine response (Fig. 8e–i), suggesting that the GRK phosphorylation-associated cellular event is a negative contributor to the overall response of epinephrine. Together, these results suggest that the GRK phosphorylation-associated cellular events contribute to the DMR of epinephrine.

#### The efficacy of distinct ligands towards the cAMP-EPAC pathway.

The activation of the  $\beta_2$ -AR is known to increase the intracellular concentration of cyclic adenosinemonophosphate (cAMP), leading to the activation of cyclic nucleotide-gated ion channels, EPAC and protein kinase A (PKA)<sup>53,54</sup>. The  $\beta_2$ -AR ligands are divergent in their ability to activate the Epac enzyme, as measured using an Epac-based cAMP sensor<sup>14</sup>. Therefore, we next examined the impact of brefeldin A and Epac1 knockdown on the DMR responses of different ligands in the subclone A. Brefeldin A, initially isolated as an anti-viral antibiotic and a known drug for activating a GTPase of a GEF (Arf1p), is also known to be an inhibitor of Epac-mediated signaling<sup>55,56</sup>. DMR profiling of the AR ligand library in the subclone A revealed an interesting modulation pattern by both

brefeldin A and Epac1 RNAi (Fig. 9). For this analysis, the DMR signals of all ligands were compared with their corresponding net changes induced by either brefeldin A or Epac1 RNAi.

Detailed analysis revealed several interesting aspects about the sensitivity of ligand-induced DMR to the Epac inhibition (Fig. 9a). First, out of sixty-nine ligands all known  $\beta_2$ -AR agonists (twenty-one in total) gave rise to a DMR signal greater than 40 pm in the untreated subclone A, suggesting that these ligands have distinct agonistic activity. Second, brefeldin A treatment and Epac1 RNAi knockdown led to comparable results for all ligands examined. However, compared to brefeldin A, Epac1 RNAi knockdown generally resulted in smaller potentiation of the DMR of ligands that were sensitive to Epac inhibition. This is consistent with the moderate efficiency ( $\sim 65\%$ ) of RNAi knockdown observed in our laboratory, although we did not directly examine the Epac1 level using western blot. Third, the DMR signals of these agonists displayed distinct sensitivity to the Epac inhibition. The Epac inhibition-induced net DMR increase was found to be the greatest for epinephrine (Fig. 9b), and be negligible for UK14, 304 (Fig. 9c). The Epac inhibition potentiated the DMR of other agonists to different degrees – it markedly increased the DMR of isoproterenol, isoetharine, and cimaterol (Fig. 9d–f, respectively), but only slightly increased the DMR of clenbuterol and salbutamol (Fig. 9g and h, respectively), and had little effect on the DMR of a small group of agonists including zinterol,





ritodrine, zilpaterol, and BRL37344 (Fig. 9a). Lastly, only two beta-blockers, labetalol and betaxolol, give rise to a detectable DMR in the brefeldin A-treated cells, with a net change greater than 40 pm compared to their corresponding DMR in the untreated cells (betaxolol in Fig. 9i). These results suggest that distinct ligands have different abilities to activate the cAMP-Epac pathway through the  $\beta_2$ -AR.

## Discussion

GPCR signaling is sensitive to cell-specific parameters including the ratio of active to inactive receptor species, the rate constant for G protein activation, and expression levels of receptors and G proteins<sup>57</sup>. Here, we systematically compared the cell phenotypic profiles of a library of sixty-nine AR ligands in the parental HEK293 cells with those in the four stable subclones bearing different expression levels of the GFP tagged  $\beta_2$ -AR. By taking advantage of the distinct receptor expression levels in the same cell background achieved through stable cloning as well as the whole cell phenotypic measure using DMR assays, several interesting findings have been revealed.

First, our results suggest for the first time that HEK293 endogenously expresses functional  $G_i$ -coupled  $\alpha_{2c}$ -AR, beside the widely reported  $G_s$ -coupled  $\beta_2$ -AR. UK14,304 seems specifically activate the  $\alpha_{2c}$ -AR, while isoproterenol specifically activates the  $\beta_2$ -AR, and epinephrine, norepinephrine and methylnorepinephrine all activate both receptors. In the parental HEK293 cells the DMR of 10  $\mu$ M epinephrine closely resembled the simple sum of its DMR in the PTx- and CTx-treated cells (Fig. 6c). Furthermore, the epinephrine DMR in the CTx-treated cells was almost identical to its DMR in the  $\beta$ -blocker-treated cells, or the DMR of UK14,304 in the untreated cells (comparing Fig. 4g and 6c with Fig. 6a, respectively). Together with the insensitivity of the DMR of isoproterenol to the PTx treatment (Fig. 6b), these results suggest that it is unlikely that a  $G_s$ -to- $G_i$  switching has occurred for either epinephrine or isoproterenol at such a high dose (10  $\mu$ M). Similarly, the DMR of epinephrine in the subclone A was dominated by the  $G_s$ -mediated signaling through the  $\beta_2$ -AR (Fig. 5 and Fig. 6f). This is significant in that it has been controversial in literature whether there is a dose-dependent switching from  $G_s$ -to- $G_i$ -mediated signaling through the activation of the  $\beta_2$ -AR in HEK293 cells<sup>58,59</sup>. The presence of functional  $G_i$ -coupled  $\alpha_{2c}$ -AR in HEK293 cells at least warrants careful interpretation of the  $\beta_2$ -AR signaling in this cell line. Furthermore, the ability to dissect the DMR of epinephrine arising from  $\alpha_{2c}$ - and  $\beta_2$ -ARs also confirms that DMR is an integrated measure of the functional consequence of ligand-receptor interactions, and  $G_s$ - and  $G_i$ -mediated signaling involves distinct compartments or routes in cells although they modulate cAMP differently<sup>40,60,61</sup>. Of note, the biphasic dose responses of both epinephrine and isoproterenol in the subclone A, but not the parental and subclone D cells, suggest that the  $\beta_2$ -AR at the high expression level may form homodimers<sup>62</sup>.

Second, the label-free cell phenotypic pharmacology of AR ligands is sensitive to receptor expression level. Out of sixty-nine ligands tested, forty-five were active in at least one of the five cell lines. Except for UK14,304 that specifically activates  $\alpha_{2c}$ -AR, all others seem act at the  $\beta_2$ -AR. For the parental and subclone A cells most antagonists did not result in clear DMR; however, for the subclones B–D having moderate expression level of the  $\beta_2$ -AR all known beta-blockers except for acebutolol triggered a clear negative DMR (Fig. 2). One possibility is that in these subclones with moderate  $\beta_2$ -AR levels these beta-blockers exhibit inverse agonist activity, while acebutolol acts as a neutral antagonist<sup>57</sup>. Also notable is that the  $\alpha_1$ -antagonist tamsulosin displayed distinct pharmacology to alter the DMR of epinephrine in the parental cell line *versus* the subclone A. This is distinct from naftopidil, although both are  $\alpha_1$ -selective antagonists. Interestingly, the two drugs were reported to exhibit different clinical features<sup>63</sup>. Of note, the pharmacology observed for the AR library ligands, with an exception of rauwolfscine, suggests that it is less likely that  $\alpha_{2c}$ - and  $\beta_2$ -ARs form heterodimers in these subclones. However,

further experiments are necessary to determine whether heterodimers are formed and contribute to the cell phenotypic pharmacology observed.

Third, the epinephrine DMR is mostly originated from  $G_s$ -mediated signaling, and is mostly associated with the remodeling of actin filaments and adhesion complexes, and to less degree microtubule remodeling, the exact of which is sensitive to the receptor expression level. RNAi knockdown results also showed that the GRK-associated receptor trafficking also contributes negatively to the epinephrine DMR, but  $\beta$ -arrestins had little or small effect on the epinephrine DMR, later of which may be in part due to the moderate efficiency of RNAi knockdown, and in part due to the fact that all assays are performed under ambient temperature.  $\beta$ -Arrestin-mediated mass redistribution may be rather slow under ambient condition, leading to unnoticed or small contribution to the overall signal. Further studies under physiological conditions may be able to address whether DMR assays can detect  $\beta$ -Arrestin-mediated signaling or not.

Fourth, distinct ligands have different efficacy to activate the Epac pathway through the  $\beta_2$ -AR. Epac1 and Epac2 proteins are two a guanine nucleotide exchange factor for the small GTPases Rap1 and Rap2, and are pivotal in controlling a number of cellular processes through sensing the cAMP levels in cells<sup>53–56</sup>. HEK293 endogenously expresses both Epac1 and Epac2<sup>64</sup>. The activation of Epac proteins by  $G_s$ -coupled receptors was reported to alter actin dynamics, microtubule network, and integrin-mediated cell adhesion<sup>65,66</sup>. Our Epac inhibition study showed that the Epac pathway inhibition or knockdown potentiated the DMR of a subset of  $\beta_2$ -AR ligands but to the different degrees, suggesting that these ligands have distinct efficacy to activate the cAMP-Epac pathway through the  $\beta_2$ -AR.

DMR assay enabled by label-free RWG biosensor offers a holistic view of the functional response of ligand-receptor interactions in cells. The resultant DMR signal is an integrated cell phenotypic response arising from the activation of a large number of, as yet often undefined, signaling pathways<sup>37,67</sup>, as revealed by the present study. The DMR analysis is often complicated by its wide pathway coverage yet limited DMR signatures, as well as receptor and pathway specificity of ligands. Although the DMR is viewed to not be the best read-out for studies of ligand bias, we here show that combining the cell system sensitivity of DMR measurements with pathway deconvolution using small probe molecules and RNAi can manifest the receptor and pathway sensitivity of a family of AR ligands in HEK293 cells.

## Methods

**Reagents.** All AR ligands were obtained from vendors specified in Supplementary Table 1. Cytochalasin D, nocodazole, brefeldin A, PF573228, vinblastine, and Y27632 were purchased from Tocris Chemical Co. (St. Louis, MO, USA). Except for epinephrine that was dissolved in water, all compounds were stocked in dimethyl sulfoxide (DMSO) at 100 mM. The AR ligand library was prepared at 10  $\mu$ M and stored at  $-80^\circ\text{C}$ . All ligands were diluted directly into the assay buffer (1 $\times$  Hanks' balanced salt buffer, 20 mM Hepes, pH 7.1; HBSS) to the indicated concentrations. CTx and PTx were obtained from Sigma Chemical Co. (St. Louis, MO, USA). Epic<sup>®</sup> 384-well biosensor fibronectin-coated microplates (Corning Incorporated, Corning, NY, USA) were used directly. All mission<sup>®</sup> pre-designed siRNAs were purchased from Sigma. For each gene, the top ranked two siRNAs or validated siRNAs were picked. siRNA ID was: SASI\_Hs01\_00100032 ( $\beta$ -arrestin1\_1), SASI\_Hs02\_00336791 ( $\beta$ -arrestin1\_2), SASI\_Hs01\_00121428 ( $\beta$ -arrestin2\_1), SASI\_Hs01\_00121429 ( $\beta$ -arrestin2\_2), SASI\_Hs01\_00039322 (GRK2\_1), SASI\_Hs01\_00039321 (GRK2\_2), SASI\_Hs02\_00339102 (GRK3\_1), SASI\_Hs01\_00025366 (GRK3\_2), SASI\_Hs02\_00304451 (GRK4\_1), SASI\_Hs01\_00217889 (GRK4\_2), SASI\_Hs01\_00197540 (GRK5\_1), SASI\_Hs01\_00197541 (GRK5\_2), SASI\_Hs01\_00082468 (GRK6\_1), SASI\_Hs01\_00082469 (GRK6\_2), and SASI\_Hs02\_00319350 (Epac1). All siRNAs (10 nmole each) were diluted using 1 ml DNase/Rnase free water to prepare 10  $\mu$ M aliquots, each in 50  $\mu$ l. The RNAi aliquots were stored in  $-20^\circ\text{C}$  up to 6 months.

**HEK- $\beta_2$ AR-GFP stable cell line generation.** The parental HEK293 cell line was obtained from American Type Cell Culture (Manassas, VA, USA), and cultured in minimum essential medium having 2 mM glutamine, 4.5 g/L glucose, 2 mM glutamine, 10% fetal bovine serum (FBS), and antibiotics. The four clones of engineered HEK293 cells bearing  $\beta_2$ AR-GFP cells were made in house and their



growth patterns were found to be similar. Briefly, HEK293 cells were transfected with human pCMV- $\beta$ 2AR-GFP plasmid (OriGene Technologies, Inc., Rockville, MD, USA) using Lipofectamine<sup>TM</sup> LTX and Plus Reagent (Invitrogen) in a 6-well cell culture plate. The cells were treated with 500  $\mu$ g/ml G418 Geneticin<sup>®</sup> (Invitrogen, Grand Island, NY, USA) the next day. After transfection for 7 days in total, the survived cells were then diluted to 1 to 2 cell/well in a 96well cell culture plate to allow clones derive from a single cell. Four stable clones with homogeneous expression level of  $\beta$ 2AR-GFP were selected by visualizing the GFP signal under a fluorescence microscope. The stable cell lines were maintained in the complete medium (that is, DMEM medium containing 10% FBS, penicillin/streptomycin, L-glutamine, and 500  $\mu$ g/ml G418). The cells were passaged at 37°C with 5% CO<sub>2</sub>. All cells were passed with trypsin/ethylenediamine-tetraacetic acid when approaching 90% confluence to provide new maintenance culture on T-75 flasks and experimental culture on the fibronectin-coated biosensor microplates.

**RNAi knockdown.** siRNA transfection was performed using the N-Ter Nanoparticle siRNA Transfection System (Sigma). Specifically, 5000 cells were first plated into each well of an Epic<sup>®</sup> 384well microplate, and cultured for 20 hours using the complete medium. Next day, 12.5  $\mu$ l 10  $\mu$ M siRNA stock solution was freshly diluted with 83.5  $\mu$ l siRNA dilution buffer, following by brief vortexing and keeping on ice. The N-ter peptide solution was also freshly prepared by adding 110  $\mu$ l N-ter peptide to 584  $\mu$ l water and brief vortexing. Afterwards, the diluted siRNA solution of 96  $\mu$ l was added to the tube containing 96  $\mu$ l the N-ter peptide dilution (1:1 ratio), followed by brief vortexing and maintaining at room temperature for 15–20 minutes to allow formation of nanoparticles. The resultant transfection solution of 192  $\mu$ l was further diluted with 2308  $\mu$ l the complete medium, followed by inverting several times to mix. After removing the cell culture medium from each well of Epic<sup>®</sup> 384well biosensor plates, 40  $\mu$ l the transfection solution was added to each well. After incubation for 24 hr, the solution was replaced with fresh the complete culture medium at 37°C/5% CO<sub>2</sub>, and the cells were further cultured for 2 days before assays. The cells treated with the transfection vehicle were used as the mock control.

**Western blotting.** HEK- $\beta$ 2AR-GFP cells cultured in 6-well plate till 80–90% confluency were lysed in 1% NP40 lysis buffer (150 mM NaCl, 25 mM Tris-HCl, pH 7.6, 1% NP-40) with the protease inhibitor cocktail (Roche Applied Science, Indianapolis, IN, USA). The cell lysate was centrifuged at 14,000 rpm for 20 min. The supernatant was then transferred to a new tube and mixed with Laemmli Sample Buffer (Bio-Rad Life Sciences, Hercules, CA, USA). The protein samples were boiled at 90°C for 5 min and stored at –20°C until use. 20  $\mu$ l of each prepared protein samples were separated on 4–15% precast Tris-HCl gel (Bio-Rad) and transferred to nitrocellulose membrane. The membrane was blocked with 5% non-fat milk in 1× TBST for 2 hours at room temperature, and then blotted with primary antibodies at 4°C overnight. The next day the membrane was washed for 5× with 1× TBST before blotted with HRP conjugated secondary antibody. Western blots were developed using the ECL kit (GE Healthcare, Piscataway, NJ, USA) on a Fujifilm Luminescent Image Analyzer LAS 3000 (Fujifilm, Valhalla, NY, USA). All antibodies were purchased from Santa Cruz Biotechnology Inc. (Dallas, Texas, USA), and include mouse  $\beta$ -arrestin-1/2 antibody (A-1) (catalog # sc-74591), rabbit GRK2 antibody (C-15) (sc-562), mouse GRK3 antibody (C-11) (sc-365197), rabbit GRK4 antibody (H-70) (sc-13079), rabbit GRK5 antibody (C-20) (sc-565), rabbit GRK6 antibody (C-20) (sc-566), and goat Epac1 antibody (C17) (sc-8880).

**Fluorescence imaging.** Both epi-fluorescence and TIRF images were carried out under ambient condition using a Zeiss Axioplan fluorescence microscope equipped with a low-noise, light-sensitive Andor iXon+ electron multiplying charge-coupled device (EM-CCD) camera (Nikon Instruments, Inc., Melville, NY, USA). The HEK- $\beta$ 2AR-GFP cells were seeded at a density of 150,000 cells per well into fibronectin coated 13-mm glass bottom wells of 24-well Mattek plates (MatTek Co., Ashland, MA, USA). After overnight culture, the confluent cells were washed and maintained in the assay vehicle, and then imaged using a 488 nm argon laser of 1 mW power, coupled with a 100×, 1.49 numerical aperture TIRF objective (Nikon) using immersion oil with  $n = 1.515$  at 23°C.

**Flow cytometry.** Once harvested  $0.5 \times 10^6$  cells were washed twice with PBS, centrifuged for 5 min at 500 g and re-suspended in 0.5 mL of PBS. Samples were analyzed on a BD FACSCalibur flow cytometer (BD Biosciences, San Jose, CA). The GFP fluorescence was counted and 30,000 events were collected per sample. Histogram overlay subtraction analysis was performed using the software provided by the supplier.

**DMR assays.** DMR assays were performed using Epic<sup>®</sup> system (Corning), which is a wavelength interrogation reader system tailored for resonant waveguide grating (RWG) biosensors in microtiter plates<sup>68</sup>. All DMR assays were performed at ambient condition (26°C) using an internal temperature-control unit. This system scans the entire microplate within 7 sec using a linear array of sixteen optical fibers, and every two scans were averaged to reduce signal noise so the final temporal resolution is about 15 sec. For RNAi knockdown, a seeding density of 5000 cells per well was used followed by the four day culture and transfection protocol as mentioned above. All other DMR measurements were performed with a seeding density of 12,000 cells per well and overnight culture. For all DMR measurements, the cell confluency was examined using light microscopy and about 95% at the time of assaying. After culturing, all cells were washed twice and maintained with the HBSS and further

incubated inside the system for 1 hr. A 2-min baseline was then established. Immediate after the compound additions using the onboard liquid handler, the cellular responses were recorded. All studies were carried out with at least three replicates. For pathway deconvolution studies, the cells were pretreated with small probe molecules for 1 hr, or 100 ng/ml PTx for overnight at 37°C, or 400 ng/ml CTx for 4 hrs at 37°C, before stimulation with ligands.

**AR ligand screening.** We screened all sixty-nine AR ligands in the five cell lines, and in the 20  $\mu$ M brefeldin A- or Epac1 RNAi-treated subclone A using the one-step DMR agonist assay<sup>23</sup>. We also screened all sixty-nine AR ligands to desensitize or block the DMR of epinephrine in either the parental HEK293 or the subclone A using the two-step desensitization/antagonist assay<sup>23</sup>. All ligands were profiled at 10  $\mu$ M with four replicates.

**Data visualization and clustering.** For each DMR the responses at the six distinct time points (3, 5, 9, 15, 30, and 45 min post stimulation) were extracted for reduction of the time dimensions. All time points refer to the stimulation duration after renormalized the responses starting from  $t_0$  (the time when the compound was added). For visualization purpose the responses were color coded to illustrate relative differences in DMR signal strength (red: positive; green: negative; black: zero). In the ligand-DMR matrix each column represents one DMR response at a particular time in a specific assay condition, and each row represents one ligand. Every row and column carries equal weight. The Ward hierarchical clustering algorithm and Euclidean distance metrics (<http://www.eisenlab.org/eisen/>) were used for clustering the results. DMSO in the vehicle, a concentration that equals to those for all ligands, is also included as a negative control. Given that the assay coefficient of variation was less than 10%, the averages of all four replicates were used for similarity analysis. All DMR signals were corrected using the corresponding in-plate negative controls.

**Statistical analysis.** DMR data were analyzed by using GraphPad Prism 5.0 (GraphPad Software Inc., San Diego, CA, USA). The EC<sub>50</sub> values were obtained by fitting the dose DMR response curves with nonlinear regression.

1. Drewsm, J. Drug discovery: a historical perspective. *Science* **287**, 1960–1964 (2000).
2. Overington, J. P., Al-Lazikani, B. & Hopkins, A. L. How many drug targets are there? *Nat. Rev. Drug Discov.* **5**, 993–996 (2006).
3. Rajagopal, S., Rajagopal, K. & Lefkowitz, R. J. Teaching old receptors new tricks: biasing seven-transmembrane receptors. *Nat. Rev. Drug Discov.* **9**, 373–386 (2010).
4. Kenakin, T. & Miller, L. J. Seven transmembrane receptors as shapeshifting proteins: the impact of allosteric modulation and functional selectivity on new drug discovery. *Pharmacol. Rev.* **62**, 265–304 (2010).
5. Urban, J. D. et al. Functional selectivity and classical concepts of quantitative pharmacology. *J. Pharmacol. Exp. Ther.* **320**, 1–13 (2007).
6. Kenakin, T. P. Biased signalling and allosteric machines: new vistas and challenges for drug discovery. *Br. J. Pharmacol.* **165**, 1659–1669 (2012).
7. Kelly, E. Efficacy and ligand bias at the  $\mu$ -opioid receptor. *Br. J. Pharmacol.* **169**, 1430–1446 (2013).
8. Seifert, R., Gether, U., Wenzel-Seifert, K. & Kobilka, B. K. Effects of guanine, inosine, and xanthine nucleotides on  $\beta$ 2-adrenergic receptor/G<sub>s</sub> interactions: evidence for multiple receptor conformations. *Mol. Pharmacol.* **56**, 348–358 (1999).
9. Azzi, M. et al.  $\beta$ -Arrestin-mediated activation of MAPK by inverse agonists reveals distinct active conformations for G protein coupled receptors. *Proc. Natl. Acad. Sci. USA* **100**, 11406–11411 (2003).
10. Baker, J. G., Hall, I. P. & Hill, S. J. Agonist and inverse agonist actions of  $\beta$ -blockers at the human  $\beta$ 2-adrenoceptor provide evidence for agonist-directed signaling. *Mol. Pharmacol.* **64**, 1357–1369 (2003).
11. Galandrin, S. & Bouvier, M. Distinct signaling profiles of  $\beta$ 1 and  $\beta$ 2 adrenergic receptor ligands toward adenylyl cyclase and mitogen-activated protein kinase reveals the pluridimensionality of efficacy. *Mol. Pharmacol.* **70**, 1575–1584 (2006).
12. Wisler, J. W. et al. A unique mechanism of beta-blocker action: carvedilol stimulates  $\beta$ -arrestin signaling. *Proc. Natl. Acad. Sci. USA* **104**, 16657–16662 (2007).
13. Kim, I. M. et al.  $\beta$ -blockers alprenolol and carvedilol stimulate  $\beta$ -arrestin-mediated EGFR transactivation. *Proc. Natl. Acad. Sci. USA* **105**, 14555–14560 (2008).
14. Drake, M. T. et al.  $\beta$ -Arrestin-biased agonism at the  $\beta$ 2-adrenergic receptor. *J. Biol. Chem.* **283**, 5669–5676 (2008).
15. Evans, B. A., Sato, M., Sarwar, M., Hutchinson, D. S. & Summers, R. J. Ligand-directed signalling at  $\beta$ 2-adrenoceptors. *Br. J. Pharmacol.* **159**, 1022–1038 (2010).
16. Reiner, S., Ambrosio, M., Hoffmann, C. & Lohse, M. J. Differential signaling of the endogenous agonists at the  $\beta$ 2-adrenergic receptor. *J. Biol. Chem.* **285**, 36188–36198 (2010).
17. Patel, C. B., Noor, N. & Rockman, H. A. Functional selectivity in adrenergic and angiotensin signaling systems. *Mol. Pharmacol.* **78**, 983–992 (2010).
18. Reiter, E., Ahn, S., Shukla, A. K. & Lefkowitz, R. J. Molecular mechanism of  $\beta$ -arrestin-biased agonism at seven-transmembrane receptors. *Ann. Rev. Pharmacol. Tox.* **52**, 179–197 (2012).



19. Brunskole, H. I. *et al.* Dissociations in the effects of  $\beta_2$ -adrenergic receptor agonists on cAMP formation and superoxide formation in human neutrophils: Support for the concept of functional selectivity. *PLoS One* **8**, e64556 (2013).
20. Fang, Y. & Ferrie, A. M. Label-free optical biosensor for ligand-directed functional selectivity acting on  $\beta_2$  adrenoceptor in living cells. *FEBS Lett.* **582**, 558–564 (2008).
21. Goral, V. *et al.* Agonist-directed desensitization of the  $\beta_2$ -adrenergic receptor. *PLoS One* **6**, e19282 (2011).
22. Stallaert, W., Dorn, J. F., van Westhuizen, E., Audet, M. & Bouvier, M. Impedance responses reveal  $\beta_2$ -adrenergic receptor signalling pluridimensionality and allow classification of ligands with distinct signalling profiles. *PLoS One* **7**, e29420 (2012).
23. Ferrie, A. M., Wang, C., Deng, H. & Fang, Y. Label-free optical biosensor with microfluidics identifies an intracellular signalling wave mediated through the  $\beta_2$ -adrenergic receptor. *Integr. Biol.* **5**, 1253–1261 (2013).
24. Kahsai, A. *et al.* Multiple ligand-specific conformations of the  $\beta_2$ -adrenergic receptor. *Nature Chem. Biol.* **7**, 692–700 (2011).
25. West, G. M. *et al.* Ligand-dependent perturbation of the conformational ensemble for the GPCR  $\beta_2$ -adrenergic receptor revealed by HDX. *Structure* **19**, 1424–1432 (2011).
26. Rasmussen, S. G. *et al.* Crystal structure of the  $\beta_2$  adrenergic receptor-G<sub>s</sub> protein complex. *Nature* **477**, 549–555 (2011).
27. Zocher, M., Fung, J. J., Kobilka, B. K. & Müller, D. J. Ligand-specific interactions modulate kinetic, energetic, and mechanical properties of the human  $\beta_2$  adrenergic receptor. *Structure* **20**, 1391–1402 (2012).
28. Liu, J. J., Horst, R., Katritch, V., Stevens, R. C. & Wüthrich, K. Biased signalling pathways in  $\beta_2$ -adrenergic receptor characterized by <sup>19</sup>F-NMR. *Science* **335**, 1106–1110 (2012).
29. Kolinski, M., Plazinska, A. & Jozwiak, K. Recent progress in understanding of structure, ligand interactions and the mechanism of activation of the  $\beta_2$ -adrenergic receptor. *Curr. Med. Chem.* **19**, 1155–1163 (2012).
30. Kofuku, Y. *et al.* Efficacy of the  $\beta_2$ -adrenergic receptor is determined by conformational equilibrium in the transmembrane region. *Nature Comm.* **3**, e1045 (2012).
31. Nygaard, R. *et al.* The dynamic process of  $\beta_2$ -adrenergic receptor activation. *Cell* **152**, 532–542 (2013).
32. Venkatakrisnan, A. J. *et al.* Molecular signatures of G-protein-coupled receptors. *Nature* **494**, 185–194 (2013).
33. Deupi, X. & Kobilka, B. K. Energy landscape as a tool to integrate GPCR structure, dynamics and function. *Physiology* **25**, 293–303 (2010).
34. Kenakin, T. The potential for selective pharmacological therapies through biased receptor signaling. *BMC Pharmacol. Tox.* **13**, 3 (2012).
35. Kenakin, T. & Christopoulos, A. Signalling bias in new drug discovery: detection, quantification and therapeutic impact. *Nat. Rev. Drug Discov.* **12**, 205–216 (2013).
36. Fang, Y., Ferrie, A. M., Fontaine, N. H., Mauro, J. & Balakrishnan, J. Resonant waveguide grating biosensor for living cell sensing. *Biophys. J.* **91**, 1925–1940 (2006).
37. Fang, Y. The development of label-free cellular assays for drug discovery. *Expert Opin. Drug Discov.* **6**, 1285–1298 (2011).
38. Fang, Y., Ferrie, A. M., Fontaine, N. H. & Yuen, P. K. Characteristics of dynamic mass redistribution of epidermal growth factor receptor signaling in living cells measured with label-free optical biosensors. *Anal. Chem.* **77**, 5720–5725 (2005).
39. Schröder, R. *et al.* Deconvolution of complex G protein-coupled receptor signaling in live cells using dynamic mass redistribution measurements. *Nat. Biotechnol.* **28**, 943–949 (2010).
40. Verrier, F. *et al.* G protein-coupled receptor signaling regulates the dynamics of a metabolic multienzyme complex. *Nature Chem. Biol.* **7**, 909–915 (2011).
41. Kenakin, T. Cellular assays as portals to seven-transmembrane receptor-based drug discovery. *Nat. Rev. Drug Discov.* **8**, 617–626 (2009).
42. Ferrie, A. M., Sun, H. & Fang, Y. Label-free integrative pharmacology on-target of drugs at the  $\beta_2$ -adrenergic receptor. *Sci. Rep.* **1**, 33 (2011).
43. Morse, M., Tran, E., Levenson, R. L. & Fang, Y. Ligand-directed functional selectivity at the mu opioid receptor revealed by label-free on-target pharmacology. *PLoS One* **6**, e25643 (2011).
44. Morse, M., Sun, H., Tran, E., Levenson, R. & Fang, Y. Label-free integrative pharmacology on-target of opioid ligands at the opioid receptor family. *BMC Pharmacol. Tox.* **14**, 17 (2013).
45. von Zastrow, M. & Kobilka, B. K. Ligand-regulated internalization and recycling of human  $\beta_2$ -adrenergic receptors between the plasma membrane and endosomes containing transferrin receptors. *J. Biol. Chem.* **267**, 3530–3538 (1992).
46. Eisen, M. B., Spellman, P. T., Brown, P. O. & Botstein, D. Cluster analysis and display of genome-wide expression patterns. *Proc. Natl. Acad. Sci. USA* **95**, 14863–14868 (1998).
47. PDSP Ki database. <http://pdsp.med.unc.edu/pdsp.php>.
48. Cecchetti, V., Schiaffella, F., Tabarrini, O. & Fravolini, A. (1,4-Benzothiazinyloxy) alkylpiperazine derivatives as potential antihypertensive agents. *Bioorg. Med. Chem. Lett.* **10**, 465–468 (2000).
49. Ruffolo, R. R. Jr. & Waddell, J. E. Receptor interactions of imidazolines. IX. Cirazoline is an  $\alpha_1$  adrenergic agonist and an  $\alpha_2$  adrenergic antagonist. *J. Pharmacol. Exp. Ther.* **222**, 29–36 (1982).
50. Zaytseva, Z. *et al.* Resonant waveguide grating biosensor-enabled label-free and fluorescence detection of cell adhesion. *Sens. Actuators B: Chem.* **188**, 1064–1072 (2013).
51. Fang, Y. Label-free receptor assays. *Drug Discov. Today Technol.* **7**, e5–e11 (2010).
52. Chen, M. *et al.* Microplate-compatible total internal reflection fluorescence microscopy for receptor pharmacology. *Appl. Phys. Lett.* **102**, 193702 (2013).
53. Bos, J. L. Epac proteins: multi-purpose cAMP targets. *Trends Biochem. Sci.* **31**, 680–686 (2006).
54. Ponsioen, B., Gloerich, M., Ritsma, L. & Rehmann, H. Direct spatial control of Epac1 by cyclic AMP. *Mol. Cell. Biol.* **29**, 2521–2531 (2009).
55. Zhong, N. & Zucker, R. S. cAMP acts on exchange protein activated by cAMP/ cAMP-regulated guanine nucleotide exchange protein to regulate transmitter release at the crayfish neuromuscular junction. *J. Neurosci.* **25**, 208–214 (2005).
56. Ster, J. *et al.* Epac mediates PACAP-dependent long-term depression in the hippocampus. *J. Physiol.* **587**, 101–113 (2009).
57. Kinzer-Ursem, T. L. & Linderman, J. J. Both ligand- and cell-specific parameters control ligand agonism in a kinetic model of G protein-coupled receptor signaling. *PLoS Comput. Biol.* **3**, e6 (2007).
58. Daaka, Y., Luttrell, L. M. & Lefkowitz, R. J. Switching of the coupling of the  $\beta_2$ -adrenergic receptor to different G proteins by protein kinase A. *Nature* **390**, 88–91 (1997).
59. Friedman, J., Babu, B. & Clark, R. B.  $\beta_2$ -Adrenergic receptor lacking the cyclic AMP-dependent protein kinase consensus sites fully activates extracellular signal-regulated kinase 1/2 in human embryonic kidney 293 cells: Lack of evidence for G<sub>s</sub>/G<sub>i</sub> switching. *Mol. Pharmacol.* **62**, 1094–1102 (2002).
60. Tran, E. & Fang, Y. Duplexed label-free G protein-coupled receptor assays for high throughput screening. *J. Biomol. Screen.* **13**, 975–985 (2008).
61. Kholodenko, B. N., Hancock, J. F. & Kolch, W. Signalling ballet in space and time. *Nat. Rev. Mol. Cell Biol.* **11**, 414–426 (2010).
62. Giraldo, J. On the fitting of binding data when receptor dimerization is suspected. *Br. J. Pharmacol.* **155**, 17–23 (2008).
63. Nishino, Y. *et al.* Comparison of two alpha-1-adrenoceptor antagonists, naftopidil and tamsulosin hydrochloride, in the treatment of lower urinary tract symptoms with benign prostatic hyperplasia: a randomized crossover study. *BJU Int.* **97**, 747–751 (2006).
64. Keiper, M. *et al.* Epac- and Ca<sup>2+</sup>-controlled activation of Ras and extracellular signal-regulated kinases by Gs-coupled receptors. *J. Biol. Chem.* **279**, 46497–46508 (2004).
65. Grandoch, M., Roscioni, S. S. & Schmidt, M. The role of Epac proteins, novel cAMP mediators, in the regulation of immune, lung and neuronal function. *Br. J. Pharmacol.* **159**, 265–284 (2010).
66. Rangarajan, S. *et al.* Cyclic AMP induces integrin-mediated cell adhesion through Epac and Rap1 upon stimulation of the  $\beta_2$ -adrenergic receptor. *J. Cell Biol.* **160**, 487–493 (2003).
67. Fang, Y. Troubleshooting and deconvoluting label-free cell phenotypic assays in drug discovery. *J. Pharmacol. Tox. Methods* **67**, 69–81 (2013).
68. Li, G., Ferrie, A. M. & Fang, Y. Label-free profiling of endogenous G protein-coupled receptors using a cell-based high throughput screening technology. *J. Assoc. Lab. Autom.* **11**, 181–187 (2006).

## Author contributions

A.M.F. conducted the most DMR assays, flow cytometry, and analyzed the data. H.S. conducted Western blot and part of the DMR assays, established the four subclones, and analyzed the data. N.Z. conducted the fluorescence imaging experiments. Y.F. conceived the idea, designed experiments, analyzed the data, and wrote the manuscript.

## Additional information

Supplementary information accompanies this paper at <http://www.nature.com/scientificreports>

**Competing financial interests:** Y.F., A.M.F. and N.Z. are employee of Corning Incorporated. DMR assay is patented. Epic® system is commercial product from Corning Incorporated.

**How to cite this article:** Ferrie, A.M., Sun, H., Zaytseva, N. & Fang, Y. Divergent Label-free Cell Phenotypic Pharmacology of Ligands at the Overexpressed  $\beta_2$ -Adrenergic Receptors. *Sci. Rep.* **4**, 3828; DOI:10.1038/srep03828 (2014).



This work is licensed under a Creative Commons Attribution-NonCommercial-ShareAlike 3.0 Unported license. To view a copy of this license, visit <http://creativecommons.org/licenses/by-nc-sa/3.0>